ACS SENSORS

pubs.acs.org/acssensors Article

Biosensor-Linked Immunosorbent Assay for the Quantification of Methionine Oxidation in Target Proteins

Hae Min Lee, Dong Wook Choi, Seahyun Kim, Aro Lee, Minseo Kim, Yeon Jin Roh, Young Ho Jo, Hwa Yeon Cho, Ho-Jae Lee, Seung-Rock Lee, Lionel Tarrago, Vadim N. Gladyshev, Ji Hyung Kim,* and Byung Cheon Lee*

Cite This: *ACS Sens.* 2022, 7, 131−141 Read Online

ACCESS | Metrics & More | Article Recommendations | Supporting Information

ABSTRACT: Methionine oxidation is involved in regulating the protein activity and often leads to protein malfunction. However, tools for quantitative analyses of protein-specific methionine oxidation are currently unavailable. In this work, we developed a biological sensor that quantifies oxidized methionine in the form of methionine-*R*-sulfoxide in target proteins. The biosensor "tpMetROG" consists of methionine sulfoxide reductase B (MsrB), circularly permuted yellow fluorescent protein (cpYFP), thioredoxin, and protein G. Protein G binds to the constant region of antibodies against target proteins, specifically capturing them. Then, MsrB reduces the oxidized methionine in these proteins, leading to cpYFP fluorescence changes. We assessed this biosensor for quantitative analysis of methionine-*R*-sulfoxide in various proteins, such as calmodulin, IDLO, LegP, Sacde, and actin. We further developed an immunosorbent assay using the biosensor to quantify methionine oxidation in specific proteins such as calmodulin in animal tissues. The biosensor-linked immunosorbent assay proves to be an indispensable tool for detecting methionine oxidation in a protein-specific manner. This is a versatile tool for studying the redox biology of methionine oxidation in proteins.

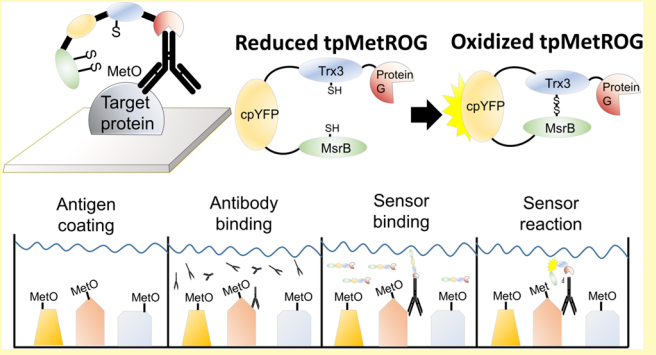

KEYWORDS: *methionine oxidation, biosensor, methionine sulfoxide reductase B, immunosorbent assay, redox*

Peroxide, superoxide, and hydroxyl radicals are highly reactive oxygen species (ROS).[1] In aerobic organisms, ROS are generated as the byproducts of the mitochondrial respiratory chain reaction, but they can also be produced during specific immune responses.[2] Accumulated ROS in cells can exert both beneficial and detrimental influence on numerous cellular events by altering the functions of various macromolecules, including proteins, lipids, and nucleic acids.[3−5] In particular, several amino acid residues in proteins can be readily oxidized by ROS. Sulfur-containing amino acids, including methionine (Met), are especially easily oxidized by ROS. Oxidation of sulfur in methionine produces either methionine-*S*-sulfoxide (MetSO) or methionine-*R*-sulfoxide (MetRO).[6] MetSO and MetRO are reduced by MsrA and methionine sulfoxide reductase B (MsrB), respectively, which are conserved in animals, including mammals.

Emerging evidence suggests that reversible oxidation/reduction of methionine residues is an adaptation for functional regulation of proteins.[7−10] Oxidation of methionine residues 281 and 282 within the regulatory region of calcium (Ca^{2+})-/calmodulin-dependent protein kinase II (CaMKII) increases its enzymatic activity even in the absence of Ca^{2+}/calmodulin.[11] Oxidation of methionine residues in hypochlorite-responsive transcription factor (HypT), a protein expressed in *Escherichia coli* (*E. coli*), induces the expression of various genes required for escaping cell death due to the oxidative stress mediated by neutrophils during an innate immune response.[12] In F-actin, the stereoselective oxidation of methionine 46 and 49 catalyzed by molecules interacting with the CasL (MICAL) family of proteins results in actin depolymerization and the generation of G-actin monomers.[13,14] These oxidized methionine residues involved in altering protein functions were shown to be reduced by either MsrA or MsrB, which brings the proteins back to the original reduced state. For example, G-actin monomers disassembled by oxidation of the two conserved methionine residues are reassembled to the F-actin polymer upon treatment with MsrB.[15,16] Additionally, oxidation of specific methionine

Received: August 25, 2021
Accepted: December 8, 2021
Published: December 22, 2021

residues in proteins may alter the protein structure, thereby diminishing the activity.[17−19]

Therefore, it can be surmised that global methionine oxidation may confer differential effects on individual protein functions. It is critical to identify proteins where methionine oxidation levels regulate protein functions. However, detecting methionine oxidation in a specific protein has been challenging due to the spontaneous oxidation that occurs during sample preparation. To eliminate this oxidation source, Sun and Anderson replaced ammonium persulfate with a flavin mononucleotide/diphenyliodonium chloride/sodium toluenesulfinic acid system and UV light.[20] Also, artificial oxidation could be distinguished by using the use of isotopes through LC−MS/MS.[21,22] However, high cost and incomplete specificity still remain the challenges to be overcome.[23,24] Recently, an advanced approach has been developed by Tarrago and his colleagues. It is a ratiometric fluorescent sensor that detects the level of global methionine oxidation *in vitro* and *in vivo*.[25] However, there is still a need for measuring the degree of methionine oxidation of a specific protein target. Here, we introduce a new method for measuring the degree of methionine oxidation in a target-specific manner based on the strategy developed from the sensor devised by Tarrago and his colleagues. Using the ability of protein G to bind immunoglobulins, we made a recombinant protein composed of yeast MsrB, circularly permuted yellow fluorescent protein (cpYFP), and yeast Trx3, followed by protein G with a short amino acid linker. The biosensor was then applied in immunosorbent assays to measure the degree of methionine oxidation of specific purified proteins from cell lysates and organ extracts.

MATERIALS AND METHODS

Construction of the Target Protein MetRO Protein G (tpMetROG) Biosensor. All polymerase chain reactions (PCRs) and site-directed mutagenesis were performed using the KOD Plus polymerase (TOYOBO, Osaka, Japan). *MsrB* and *Trx3* were amplified from the *Saccharomyces cerevisiae* genomic DNA using PCR with a specific pair of primers (listed in Table S1) containing overlapping extensions for *cpYFP*. *cpYFP* was amplified from the H_2O_2 sensor, HyPer,[26] using PCR with a specific pair of primers (listed in Table S1). A *flexible linker* and *protein G* were *de novo* synthesized (listed in Table S2) from Cosmogenetech (South Korea). *MsrB* and *Trx3* amplicons were subsequently fused to *cpYFP* by PCR. Sequentially, the *flexible linker* and *protein G* were fused to the C terminal of Trx3 by PCR with a specific pair of primers (listed in Table S1). The fused MsrB/cpYFP/Trx3/flexible linker/protein G was purified using a PCR/gel purification kit (Bioneer, Daejeon, Republic of Korea). For the construction of the MsrB/cpYFP/Trx3/flexible linker/protein G expression plasmid, purified fragments were proportionally mixed with the pET 21a cloning vector (Addgene, MA, USA) plasmid that was previously digested by the *Bam*HI and *Xho*I restriction enzymes (Thermo Fisher Scientific, MA, USA) and further ligated using T4 DNA ligase (Invitrogen, MA, USA). Then, the ligation mixture was transformed into *E. coli* DH5α (Invitrogen, MA, USA) for the selection and amplification of the correct recombinant plasmid.

Expression and Purification of tpMetROG and Methionine-Rich Proteins. All constructed plasmids were introduced into *E. coli* Rosetta2 (DE3) (Novagen, WI, USA) grown in Luria−Bertani medium (Formedium, Norfolk, England) containing ampicillin (50 μg/mL) at 37 °C. When absorption at 600 nm (A_{600}) reached ∼0.6, the synthesis of the recombinant protein was induced by adding 100 μM isopropyl β-D-1-thiogalactopyranoside (Gold Biotechnology, MO, USA) at 18 °C. After 18−24 h of incubation, the cells were collected by centrifugation at 3000*g* for 30 min. Pellets were resuspended in buffer A (50 mM Tris-HCl, 150 mM NaCl, 5 mM 2-mercaptoethanol, and pH 8.0) and subsequently sonicated. Proteins were purified using the HisTrap HP column (GE Healthcare, IL, USA) and eluted with buffer B (buffer A supplement 500 mM imidazole). Protein solutions were concentrated using Amicon Ultra-15 30 kDa centrifugal filters (Millipore, MA, USA). The initial protein concentrations were measured using the Pierce bicinchoninic acid (BCA) protein kit (Thermo Scientific, MA, USA). The recombinant proteins were aliquoted and stored at −80 °C.

For the analysis of methionine-rich proteins (MRPs), we selected four proteins, including IDLO from *Idiomarina loihiensis* L2TR, Sacde from *Saccharophagus degradans* 2−40, LegP from *Legionella pneumophila* (LegP), and calmodulin from *Mus musculus*.[27] All proteins were prepared as His-tag forms using a pET-21a(+) cloning vector (Novagen, WI, USA). All constructed plasmids were introduced into *E. coli* Rosetta2 (DE3) (Novagen, WI, USA) grown in Luria−Bertani medium containing ampicillin (50 μg/mL) at 37 °C. Purification was carried out similarly as described above.

Spectroscopic Characterization of tpMetROG Biosensors with Oxidized MRPs. For assessing the tpMetROG biosensor, purified proteins (10−20 μM) were reduced using 10 mM dithiothreitol (DTT) at room temperature for 30 min. After reduction, the proteins were desalted using HiTrap Desalting columns (GE Healthcare, IL, USA) in 50 mM Tris-HCl, pH 7.5, and were diluted to 1−5 μM in the same buffer for recording the fluorescence. The purified MRPs (calmodulin, IDLO, LegP, Sacde) were oxidized using 40 mM hydrogen peroxide (H_2O_2) at room temperature for 2 h. Residual H_2O_2 was removed by centrifugation (14,000*g*, 10 min, 4 °C) using an Amicon Ultra-0.5 centrifugal filter with 10 K cutoffs. The centrifugation step was repeated five times. The protein concentrations were measured using the Pierce BCA protein kit (Thermo Scientific, MA, USA). The fully reduced tpMetROG (1 μM) in the working buffer (50 mM Tris-HCl, 150 mM NaCl, and pH 7.5) was incubated with an MRP (1−2 μM), partially oxidized MRP (1−2 μM), at room temperature for 30 min. The fully oxidized tpMetROG (1 μM) was prepared by incubating the fully reduced tpMetROG with *N*-acetyl methionine sulfoxide (100 μM) at room temperature for 30 min. Methionine (Met) and methionine sulfoxide (MetO) (Sigma-Aldrich, MO, USA) were prepared in 1 mM in 50 mM Tris-HCl (pH 8.0). The fully reduced tpMetROG was incubated with Met (100 μM) or MetO (100 μM) at room temperature for 30 min.

The fluorescence spectrum is recorded in Costar black clear-bottom 96-well microplates using SpectraMax I3 (Molecular Devices, CA, USA). Absorbance spectra were recorded from 360 to 800 nm in a 1 nm step increment. Excitation spectra were recorded from 380 to 510 nm with a 535 nm emission and a 530 nm cutoff in a 1 nm step increment. The device was typically set to 10 reads per well with the photomultiplier tube set on "auto". Emission spectra were recorded from 500 to 750 nm with an excitation wavelength of 410 nm in a 1 nm step increment. The normalized fluorescence intensity (NFI) was obtained by dividing all spectrum values by the maximum value recorded at a 535 nm emission wavelength. The percentage of oxidized tpMetROG was represented as relative fluorescence intensity (RFI), and RFI was determined using the following equation (eq 1):

$$\text{RFI of tpMetROG} = (R_{\text{reduced}} - R)/(R_{\text{reduced}} - R_{\text{oxidized}}) \quad (1)$$

where R is measured by the $F_{500\text{nm}}/F_{415\text{nm}}$ ratio of the excitation spectrum. R_{reduced} is the $F_{500\text{nm}}/F_{415\text{nm}}$ ratio of the fully reduced tpMetROG and R_{oxidized} is the $F_{500\text{nm}}/F_{415\text{nm}}$ ratio of the fully oxidized tpMetROG.[28]

pH Calibration and Kinetic Measurement. For analyzing the pH influence, the following buffers were used: 50 mM phosphate, 150 mM NaCl (pH 5.8, 6.4, and 7.0), and 50 mM Tris-HCl, 150 mM NaCl (pH 7.5, 8.0, 8.3, and 9.0). The fully reduced tpMetROG (1 μM) or the inactive tpMetROG (1 μM) was incubated with IDLO (2 μM) or oxidized IDLO (2 μM) in a Costar black clear-bottom 96-well microplate for 30 min at 37 °C. The fluorescence spectrum is recorded using the SpectraMax I3 (Molecular Devices, CA, USA). The fluorescence ratio [FR ($F_{500\text{nm}}/F_{415\text{nm}}$)] was calculated as the

https://doi.org/10.1021/acssensors.1c01819
ACS Sens. 2022, 7, 131−141

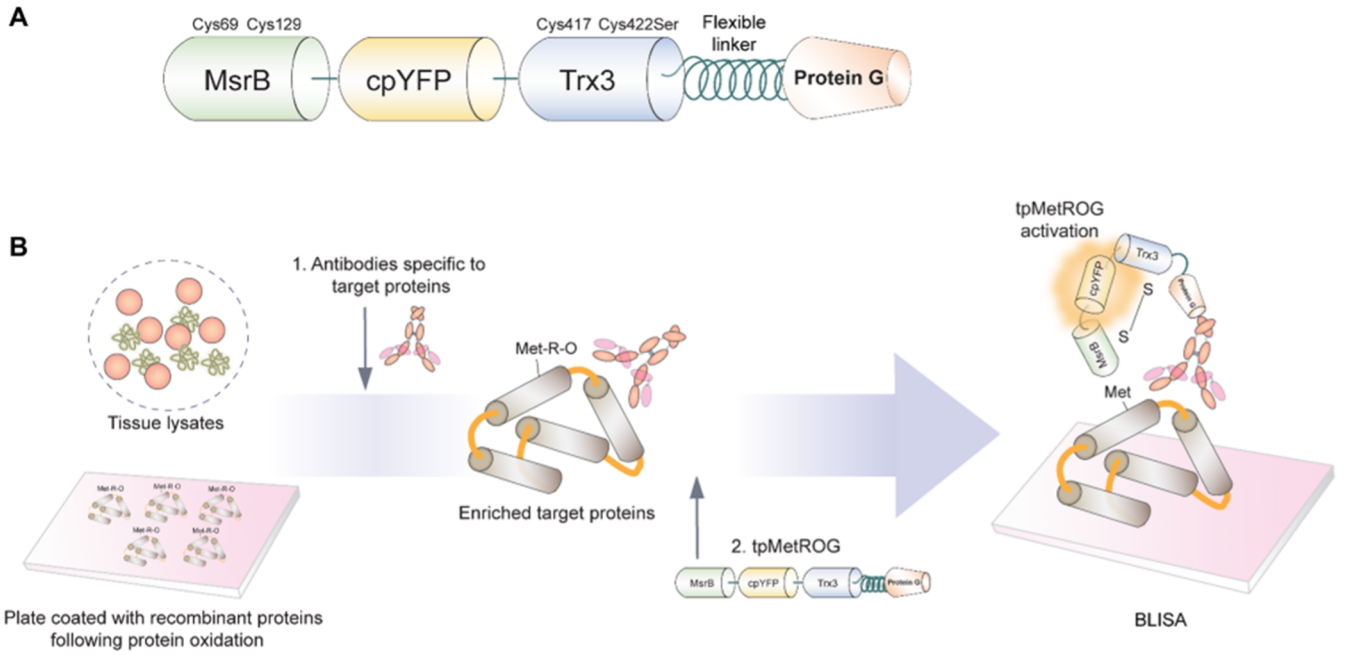

Figure 1. Schematic representation of the tpMetROG biosensor and its application in the immunosorbent assay. (A) Schematic representation of the tpMetROG biosensor construct encoding *cpYFP* flanked by *MsrB1* and *Trx3* at the N- and C-terminus and *protein G* linked to the C-terminus of *Trx3* by a peptide linker. (B) Schematic representation of the biosensor-linked immunosorbent assay (BLISA) using tpMetROG. First, the plate is coated with the protein or a sample containing a protein to measure the oxidation state of methionine. After adding the primary antibody for a target protein, the unbound antibody is washed away, and tpMetROG is added at low temperature. The unbound tpMetROG is washed using the working buffer. After incubation at 37 °C, the tpMetROG fluorescence spectrum was recorded.

ratio of fluorescence at 500 and 415 nm for the excitation spectrum with an emission wavelength of 535 nm.

For measuring the kinetic reactivity of tpMetROG with various substrates, the reduced biosensor (1 μM) was incubated for 60 min with buffer A (50 mM Tris-HCl, 150 mM NaCl, and pH 7.5), DTT (1 mM), oxidized calmodulin (2 μM), or reduced calmodulin (2 μM) as control. The examination of the excitation spectrum and the calculation of F_{500nm}/F_{415nm} were performed as described above. The F_{500nm}/F_{415nm} (R) ratio was normalized to the value at t = 0 (R_0).

Application of tpMetROG Using Purified MRPs in Antibody-Based Immunoassays. tpMetROG was applied in antibody-based immunoassays. Purified MRPs were oxidized with 10−40 mM hydrogen peroxide (H_2O_2) at room temperature for 2 h. Residual H_2O_2 was removed by repeating five cycles of washing and centrifugation (14,000g, 10 min, and 4 °C) using an Amicon Ultra-0.5 centrifugal filter with 10 K cutoffs. The protein concentrations were measured using the Pierce BCA protein kit (Thermo Scientific, MA, USA). The MRPs were prepared at 2 μM in 200 μL buffer A. Black immunoplates (SPL Life Sciences, Korea) were coated with MRPs for 2 h at room temperature and then blocked with a SuperBlock (Thermo Scientific, MA, USA). Dilutions of anti-IDLO (1:1000; Convance), anti-Sacde (1:1000; Convance), anti-LegP (1:1000; Convance), or anti-calmodulin (1:1000; Convance) antibodies were added to the plates for 2 h at room temperature. After washing with a wash buffer (100 mM phosphate, 150 mM sodium chloride, 0.05% Tween 20, and pH 7.2), the plates were incubated with the fully reduced tpMetROG (1 μM) in 200 μL working buffer (50 mM Tris, 150 mM NaCl, pH 7.5) for 2 h at 18 °C. After washing the plates again with the working buffer, 200 μL of working buffer was added and incubated at 37 °C for 30 min. Then, fluorescence was recorded using a SpectraMax I3. The excitation spectrum was recorded from 380 to 510 nm with a 535 nm emission and a 530 nm cutoff in a 1 nm increment. The percentage of oxidized tpMetROG is represented as RFI.

Application of tpMetROG Using Whole Cell Lysates. tpMetROG was used to analyze the oxidation of calmodulin obtained from the lysates of Raw264.7 and U87MG cells. Raw264.7 cells were cultured in HyClone RPMI 1640 medium (Thermo Fisher Scientific, MA, USA) supplemented with 10% fetal bovine serum (FBS), penicillin 100 U/mL, and 100 μg/mL streptomycin. U87MG cells were cultured in HyClone Dulbecco's modified Eagle's medium (Thermo Fisher Scientific, MA, USA) supplemented with 10% FBS, 100 U/mL penicillin, and 100 μg/mL streptomycin. The cells were oxidized with 15, 30, and 45 mM H_2O_2 for 40 min at 37 °C, or 5, 10, and 15 mM NaOCl for 15 min at 37 °C, or with 100 ng/mL lipopolysaccharides (LPS) for 6−16 h. After the treatment, the cells were washed three times with cold phosphate-buffered saline (PBS), and the harvested cells were recovered by centrifugation. The cells were lysed in RIPA buffer [30 mM *N*-(2-hydroxyethyl)piperazine-*N*′-ethanesulfonic acid, pH 7.3, containing 150 mM NaCl, 0.1% (w/v) sodium dodecyl sulfate, 1% (v/v) Triton X-100, and 1% (w/v) Na-deoxycholate], and the lysates were centrifuged at 16,000g for 10 min at 4 °C. The protein concentrations of the supernatant were measured using the Pierce BCA protein kit. The same amount of total protein (1.6 mg/mL, 200 μL) was coated on Black immunoplates, incubated for 2 h at room temperature, and blocked with the SuperBlock. A dilution of anti-calmodulin antibodies (1:1000; Convance) was applied for 2 h at room temperature. After washing with a wash buffer (100 mM phosphate, 150 mM sodium chloride, 0.05% Tween 20, and pH 7.2), the plates were incubated with the fully reduced tpMetROG (1 μM) in 200 μL working buffer (50 mM Tris, 150 mM NaCl, and pH 7.5) for 2 h at 18 °C. After the plates were washed again with the working buffer, 200 μL of working buffer was added and incubated at 37 °C for 30 min. Then, the fluorescence was recorded in the same manner as described above.

Quantification of Oxidized Methionine from Mouse Tissues Using tpMetROG. All animal experiments were approved by the Institutional Animal Care and Use Committee (IACUC) of Korea University (KUIACUC-2019-0107). MsrB1 knockout (10−12 weeks old)[29] and age- and sex-matched C57BL/6J (Orient Bio) mice were used in this study. Mice were anesthetized by intraperitoneal injection of sterile avertin (tribromoethanol: 200 mg/10 mL/kg) and euthanized by cervical dislocation. The small intestine, large intestine, brain, heart, liver, kidneys, and lungs were dissected under sterile

https://doi.org/10.1021/acssensors.1c01819
ACS Sens. 2022, 7, 131−141

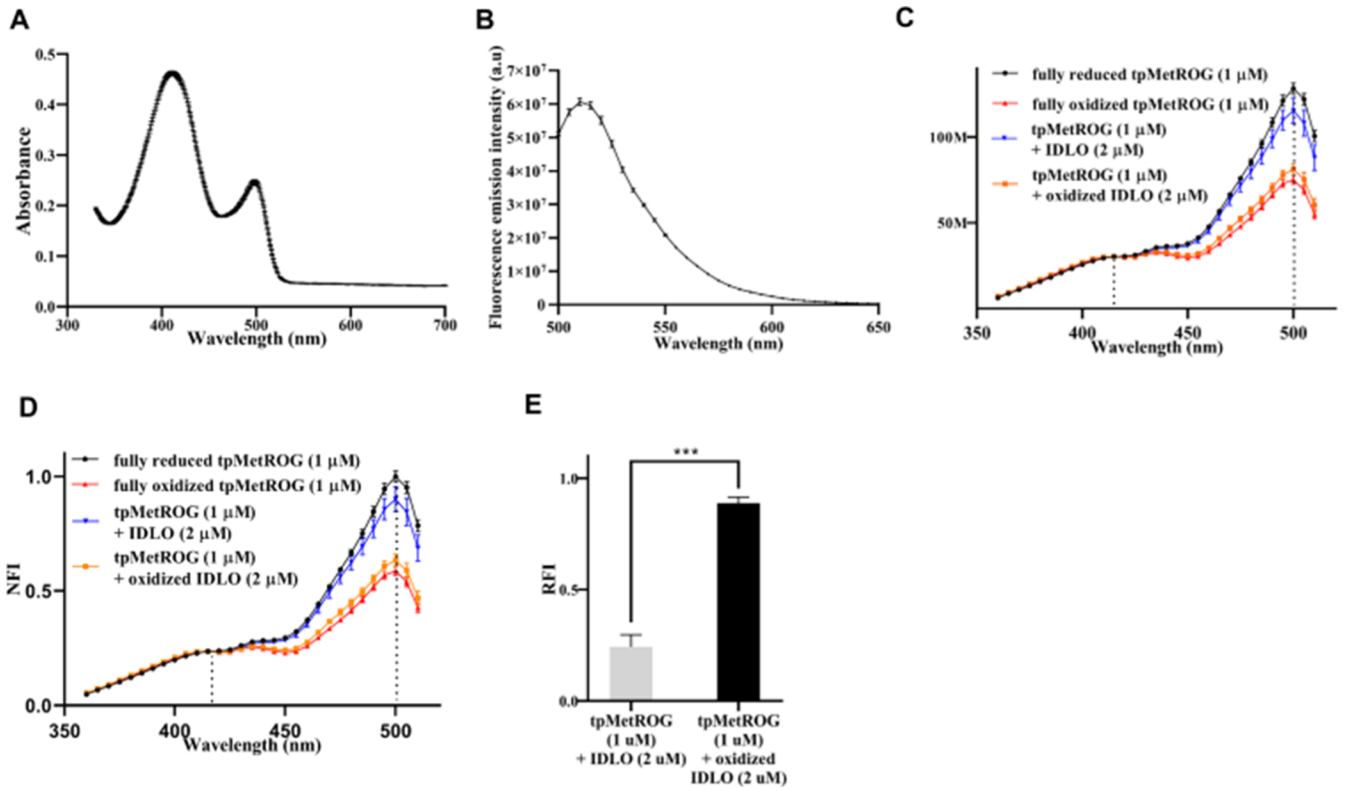

Figure 2. Optical spectral analysis of the tpMetROG sensor. (A) Absorption spectrum of reduced tpMetROG. (B) Emission spectrum of reduced tpMetROG (1 μM) when the maximum absorbance wavelength (410 nm) was used as the excitation wavelength. (C) Excitation spectrum and (D) NFI of the fully reduced tpMetROG (1 μM) incubated with or without IDLO (2 μM), partially oxidized IDLO, or *N*-acetyl methionine sulfoxide (100 μM) when the emission wavelength was fixed at 535 nm. The dotted vertical lines indicate the 415 and 500 nm emission. (E) Relative fluorescence intensity (RFI) of tpMetROG (1 μM) incubated with IDLO (2 μM) or partially oxidized IDLO (2 μM). Data are presented as means ± SD and are representative of three replicates. ***$p < 0.001$, as determined by the two-tailed paired *t*-test.

conditions. Each organ was immediately rinsed with PBS and weighed. Each organ was placed in a 15 mL polystyrene tube containing 2 mL of 0.2% Tween 20/TBS and homogenized on ice with a Polytron PT1200E homogenizer (Kinematica AG, Luzern, Switzerland). The homogenates were centrifuged at 16,000*g* for 10 min at 4 °C. The protein concentration of the supernatants was measured using the Pierce BCA protein kit. The same amount of total protein (3.2 mg/mL, 200 μL) was coated into black immunoplates and incubated for 2 h at room temperature and then blocked with the SuperBlock. Anti-calmodulin (1:1000; Convance) antibodies were applied for 2 h at room temperature. After washing with a wash buffer (100 mM phosphate, 150 mM sodium chloride, 0.05% Tween 20, and pH 7.2), the plates were incubated with the fully reduced tpMetROG (1 μM) in 200 μL working buffer (50 mM Tris, 150 mM NaCl, and pH 7.5) for 2 h at 18 °C. After washing the plates again with the working buffer, 200 μL of working buffer was added and incubated at 37 °C for 30 min. Then, fluorescence was recorded in the same manner as described above.

Analysis of Stereospecific Oxidation in F-Actin Using tpMetROG. Recombinant mouse MICAL1 and the oxidized form of F-actin were prepared as described previously.[30] MICAL1-oxidized F-actin and actin were coated on black immunoplates and incubated for 2 h at room temperature and then blocked with the SuperBlock. A proper dilution of mouse monoclonal anti-β actin antibody (1:1000) (Santa Cruz Biotechnology, TX, USA) was applied for 2 h at room temperature. After washing with a wash buffer (100 mM phosphate, 150 mM sodium chloride, 0.05% Tween 20, and pH 7.2), the plates were incubated with the fully reduced tpMetROG (1 μM) in 200 μL working buffer (50 mM Tris, 150 mM NaCl, and pH 7.5) for 2 h at 18 °C. After washing the plates again with the working buffer, 200 μL of working buffer was added and incubated at 37 °C for 30 min. Then, the fluorescence was recorded in the same manner as described above.

Statistical Analysis. Data are presented as mean ± standard error. To compare two groups, the two-tailed unpaired *t*-test, Mann−Whitney test, or Wilcoxon test was used with or without the assumption of normality. The number of asterisks indicates the degree of statistical significance according to the *p*-value. All statistical analyses were calculated using Prism 8 software (GraphPad Software, CA, USA).

RESULTS

Construction of a Biosensor Detecting the Oxidation State of Methionine Residues in Target Proteins. We prepared a fusion protein named tpMetROG, consisting of MsrB, cpYFP, and thioredoxin3 (Trx3), a peptide linker, and protein G in succession (Figure 1A). Protein G is a cell surface protein from *Streptococci*, and its B1 domain binds to the Fc region of immunoglobulin G.[25,31] Once the biosensor reacts with MetRO, a stable disulfide bond is formed between MsrB and Trx3, causing changes in the spectral properties of cpYFP: (1) reduction of the methionine *R*-sulfoxide residue of a target protein leads to the formation of sulfenic acid on catalytic cysteine (Cys129) of MsrB, (2) the resolving cysteine (Cys69) in proximity attacks the sulfenic acid intermediate to form an intramolecular disulfide, reducing the sulfenic acid content, (3) the disulfide bond between two cysteines is reduced by Trx3 by a similar mechanism as in (2), resulting in the formation of a transient intermolecular bond between Cys69 of MsrB and Cys417 of Trx3. In our recombinant Trx3, the resolving cysteine (Cys422) has been substituted to serine, which makes the transient disulfide bond between MsrB and Trx3 stable,

https://doi.org/10.1021/acssensors.1c01819
ACS Sens. 2022, 7, 131−141

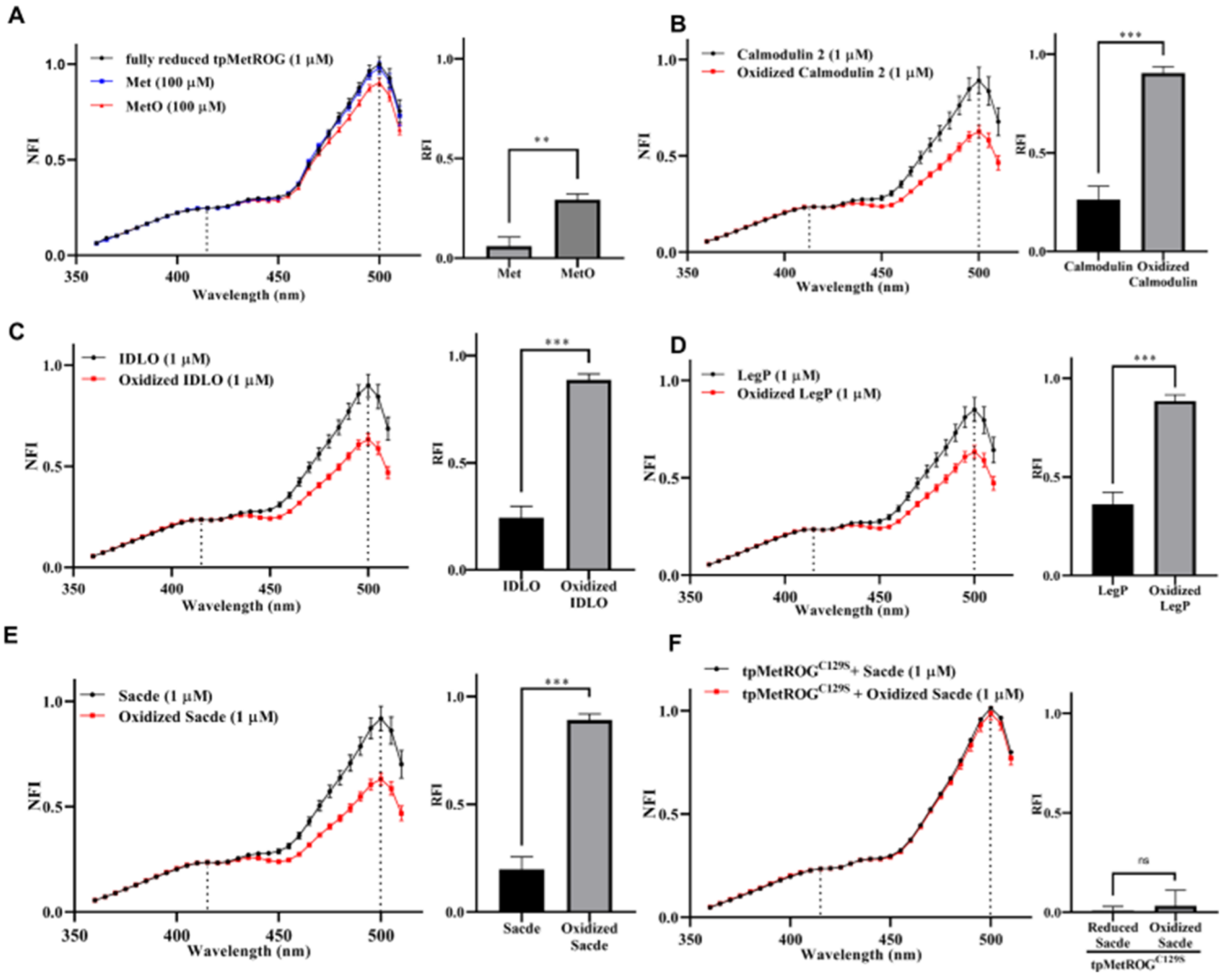

Figure 3. Analysis of various MRPs using tpMetROG. (A) NFI and relative fluorescence intensity (RFI) of reduced tpMetROG (1 μM) incubated with methionine (Met, 10 μM) or methionine sulfoxide (MetO, 10 μM) when the emission wavelength was fixed at 535 nm. (B) NFI and RFI of reduced tpMetROG (1 μM) incubated with (B) calmodulin (1 μM) or partially oxidized calmodulin (1 μM), (C) IDLO (1 μM) or partially oxidized IDLO (1 μM), (D) LegP (1 μM) or partially oxidized LegP (1 μM), and (E) Sacde (1 μM) or partially oxidized Sacde (1 μM) when emission wavelength was fixed at 535 nm. (F) NFI and RFI of inactive mutant tpMetROG^{C129S} incubated with Sacde (1 μM) or partially oxidized Sacde (1 μM) when the emission wavelength was fixed at 535 nm. The dotted vertical lines indicate the 415 and 500 nm. Data are presented as means ± SD and are representative of three replicates. $^{**}p < 0.01$ and $^{***}p < 0.001$; ns, not significant, as determined by the two-tailed paired *t*-test.

thereby affecting the structure of cpYFP permanently.[25,28,32] Importantly, this tpMetROG biosensor is designed to bind to the Fc region *via* protein G, allowing it to detect methionine sulfoxide in a protein-specific manner using antibodies (Figure 1B). Using the sensing ability of tpMetROG, we designed a method named BLISA, similar to indirect ELISA (Figure 1B), as follows: (1) coating proteins from the tissue lysates on the plate, (2) adding the primary antibody for a target protein, (3) washing away the unbound antibody and then adding tpMetROG at low temperature, (4) washing away the unbound tpMetROG and then adding the working buffer with increasing temperature, and (5) measuring the change of fluorescence intensity in response to the reduction of methionine sulfoxide of a target protein.

Optical Properties of tpMetROG. When purified tpMetROG was analyzed for absorbance spectra, two peaks appeared at 410 and 500 nm (Figure 2A). The purified tpMetROG showed a single peak at 515 nm in the emission spectrum (Figure 2B) and two peaks at 415 and 500 nm in the excitation spectrum (Figure 2C). To characterize the optical properties of tpMetROG and the changes upon Met oxidation, the excitation spectrum was analyzed by incubating tpMetROG with or without partially oxidized, fully oxidized, or untreated IDLO. For readability, we used the NFI of the excitation spectrum (Figure 2D) calculated by dividing all the excitation spectrum values by the maximum value of the excitation spectrum. Indeed, the NFIs of tpMetROG at 500 nm decreased after reacting with the fully or partially oxidized IDLO, but the NFIs at 415 nm were not changed. The NFIs at 500 nm showed the greatest difference for all the tested samples, and the NFIs at 415 nm were constant (Figure 2D). Based on this observation, the NFI at both wavelengths were selected to calculate a RFI by dividing the 500 nm value by the 415 nm value to quantify methionine oxidation (see the Materials and Methods section). The RFI increased quantitatively after incubation with the oxidized IDLO,

https://doi.org/10.1021/acssensors.1c01819
ACS Sens. 2022, 7, 131−141

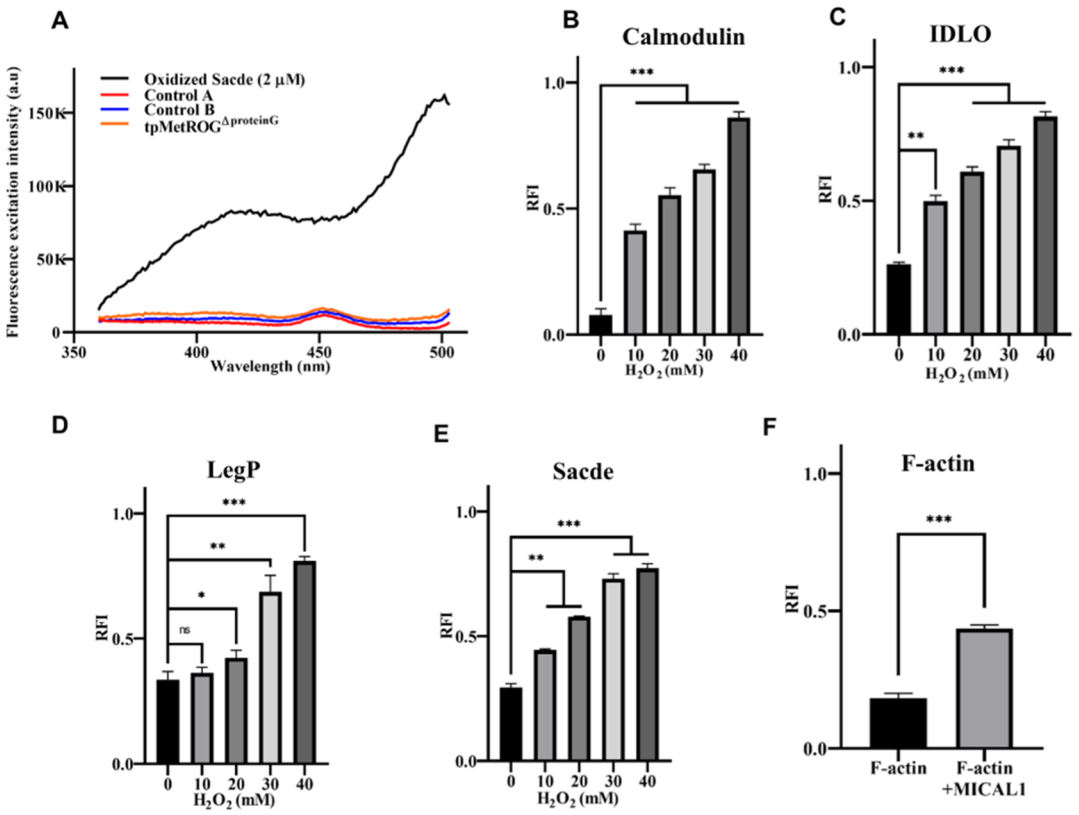

Figure 4. Characterization of tpMetROG used in immunosorbent assays. (A) Fluorescence excitation intensity of tpMetROG was measured after tpMetROG was incubated with antibodies in the Sacde-coated plate. Control A: tpMetROG incubated with the anti-Sacde antibody in a non-coated plate. Control B: tpMetROG incubated in the Sacde-coated plate without the antibody. tpMetROG$^{\Delta proteinG}$; tpMetROG lacking protein G incubated with antibodies in the Sacde-coated plate. (B−F) Relative fluorescence intensity (RFI) of tpMetROG after tpMetROG was incubated with antibodies in a plate coated with purified protein. RFIs were obtained from the excitation spectrum recorded with a 535 nm emission wavelength according to the oxidation state of calmodulin, IDLO, LegP, or Sacde. (F) Detection of stereospecific oxidation states of MICAL1-oxidized actin using tpMetROG. Static measurements of fluorescence in MICAL1-oxidized actin using tpMetROG. Actin oxidized by MICAL1 (0.2 μM) for 2 h was coated on a plate and incubated with the mouse monoclonal anti-β actin antibody, and the RFI of tpMetROG in the immunoassay after oxidation was measured. Data are presented as means ± SD and are representative of three replicates. *p < 0.05, **p < 0.01, and ***p < 0.001; ns, not significant, as determined by the two-tailed paired t-test.

reflecting the degree of protein methionine oxidation (Figure 2E).

Characterization of tpMetROG with Various Oxidized MRPs. To examine whether tpMetROG can be used as a biosensor for various proteins, the purified tpMetROG was incubated with free MetRO and oxidized MRPs. The spectrum of the NFI obtained by incubating tpMetROG with Met was similar to that obtained after incubating tpMetROG without any substrate. However, a slight reduction was observed at 500 nm in the NFI when the biosensor was incubated with free MetRO (Figure 3A). Accordingly, the RFI also showed a slight increase, suggesting that tpMetROG senses free MetRO with low efficiency (Figure 3A). Next, a significant reduction in the NFIs at 500 nm and an increase in the RFIs were observed when tpMetROG was incubated with several oxidized MRPs such as mouse calmodulin, hypothetical protein (accession no. YP_155605) from *I. loihiensis* L2TR (IDLO), and hypothetical protein (accession no. YP_095088) from *Legionella* (Figure 3B−E). Finally, there were no changes in the NFI at 500 nm and the RFI when mutated tpMetROGC129S (cysteine in the catalytic part of MsrB replaced by serine) was incubated with the oxidized Sacde (Figure 3F). Collectively, these results indicate that tpMetROG can quantitatively measure the methionine oxidation in proteins. Next, we measured the kinetic change in the biosensor to determine the optimal incubation time with the substrate. tpMetROG was incubated with calmodulin (2 μM), oxidized calmodulin (2 μM), or DTT (1 mM) for 1500 s. Then, the RFIs after every 30 s (R) were normalized to the RFI at t = 0 (R_0) and are presented as R/R_0 (Figure S1A). A rapid decrease and increase of R/R_0 were observed up to 150 s in the reaction with oxidized calmodulin and DTT. After 150 s, R/R_0 reaches a stable plateau until the end of the reaction, indicating that incubation for 150 s could be sufficient to obtain a stable RFI value (Figure S1A). We examined the effect of pH on tpMetROG activity. The FR was recorded, while tpMetROG or tpMetROG^{C129S} was incubated with reduced or oxidized IDLO in the buffers with different pH values (5.8−9.0) (Figure S1B). The fluorescence intensity (FI, F_{500nm}/F_{415nm}) of all used sensors increases to the same level with the increase of pH. In particular, tpMetROG^{C129S} with reduced IDLO, tpMetROG^{C129S} with oxidized IDLO, and tpMetROG with reduced IDLO show the same value and increased rate with the increase of pH. Accordingly, this data supports the idea that tpMetROG^{C129S} can be used as a control dead mutant to determine the pH dependency of tpMetROG under variable pH conditions. However, *in vitro* BLISA assays are performed at controlled pH by using the working buffer (50 mM Tris, 150 mM NaCl, and pH 7.5) (see the Materials

https://doi.org/10.1021/acssensors.1c01819
ACS Sens. 2022, 7, 131−141

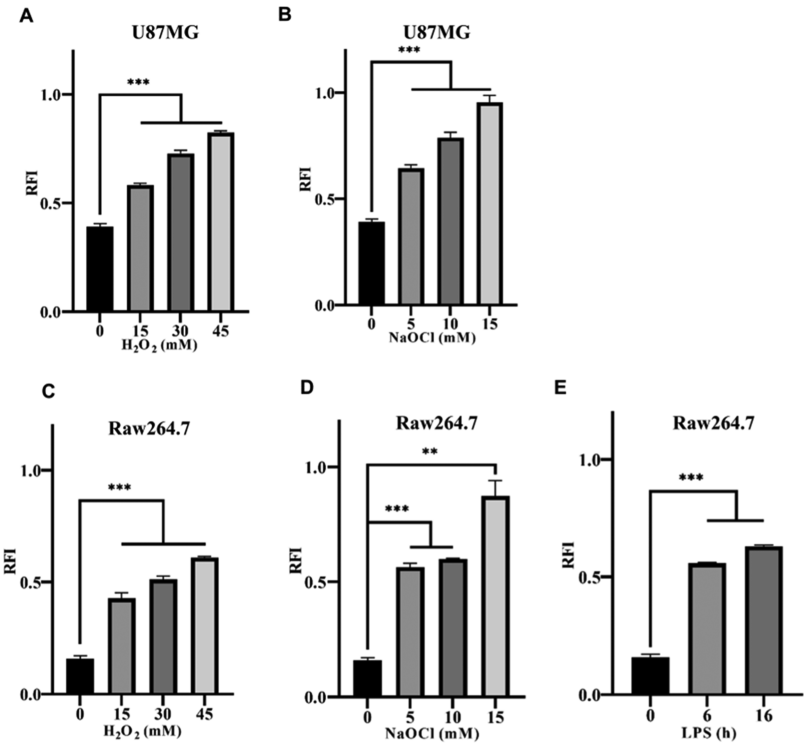

Figure 5. Quantitative analysis of calmodulin methionine oxidation in cell lysates. Relative fluorescence intensity (RFI) of tpMetROG after tpMetROG was incubated with antibodies in the plate coated with U87MG and Raw264.7 cell lysates. (A–D) RFI of tpMetROG in the immunoassay with oxidized cell lysates. U87MG or Raw264.7 cells were treated with H_2O_2 (0, 15, 30, and 45 mM, A,B) or NaOCl (0, 5, 10, and 15 mM, C,D) for 45 min (H_2O_2) or 15 min (NaOCl). Cell lysates were coated in a plate, incubated with an anti-calmodulin (1:1000; Covance) antibody, followed by sensing using tpMetROG. (E) RFI of tpMetROG in the immunoassay with LPS-treated Raw264.7 cell lysates. Lysates from Raw264.7 cells treated with 100 ng/mL LPS for 0, 6, or 16 h were used to quantify the methionine oxidation of calmodulin. Data are presented as means ± SD and are representative of three replicates. $^{**}p < 0.01$ and $^{***}p < 0.001$; ns, not significant, as determined by the two-tailed paired *t*-test.

and Methods section). Thus, the control dead mutant does not need to be applied for BLISA to determine the pH dependency. Nevertheless, *in vivo* application of tpMetROG needs to consider pH variation, and so, this control dead mutant will be a useful tool to determine the pH dependency of fluorescence intensity.

Application of tpMetROG in the Immunosorbent Assay for Purified Proteins. Indirect ELISA intends to quantify a specific protein antigen, which requires primary and enzyme-labeled secondary antibodies. The tpMetROG biosensor was applied to develop a novel method, BLISA, a modified version of indirect ELISA. The biosensor (instead of a specific protein antigen) that has an affinity for the constant region of the primary antibody replaces the enzyme-labeled secondary antibody to quantify the methionine oxidation of a specific protein. Before applying it to various protein substrates, we performed control experiments to examine non-specific interactions (Figure 4A). For the oxidized Sacde, the biosensor was pneumophila (LegP) and a hypothetical protein (accession no. YP_527410) from *S. degradans* (Sacde) incubated with anti-Sacde antibody in the oxidized Sacde-coated plate. In the control A experiment, the biosensor was incubated with an anti-Sacde antibody in a non-coated plate, and in the control B experiment, the biosensor was incubated with oxidized Sacde without anti-Sacde antibody. The experiments with tpMetROG$^{\Delta proteinG}$ indicate that the sensor lacking protein G was incubated with an anti-Sacde antibody in the oxidized Sacde-coated plate (Figure 4A). The NFIs, including the value at 500 nm, of control A, control B, and tpMetROG$^{\Delta proteinG}$ were almost similar to the basal level, whereas the NFI of the oxidized Sacde showed a dramatic increase, indicating that the tpMetROG biosensor could successfully detect methionine oxidation in a specific protein during BLISA. Therefore, it shows a successful development of functional BLISA to analyze the methionine oxidation of a specific protein without any experimental noise.

Next, we applied BLISA to various protein substrates with various oxidation levels; calmodulin, IDLO, LegP, and Sacde were oxidized by short-term exposure to H_2O_2 (10, 20, 30, and 40 mM) and used to coat plates. The RFI for all proteins [calmodulin (Figure 4B), IDLO (Figure 4C), LegP (Figure 4D), and Sacde (Figure 4E)] gradually increased as the concentration of H_2O_2 used to oxidize proteins increased. Finally, we applied BLISA to the active MICAL1-treated F-actin. Active MICAL1 contains flavin-containing monooxygenase and calponin homology domain, which stereoselectively oxidize the two conserved methionine residues of F-actin to MetRO.[16,30] As a result, the active MICAL1-treated F-actin shows increased RFI compared to the untreated F-actin (Figure 4F). Taken together, these results prove that BLISA using tpMetROG can be applied to detect methionine oxidation in a protein-specific manner.

Analysis of Methionine Oxidation of Calmodulin in Cells Using BLISA. We examined methionine oxidation of calmodulin in cells using BLISA after the induction of oxidative stress. Human glioblastoma U87MG cells (Figure 5A,B) and

https://doi.org/10.1021/acssensors.1c01819
ACS Sens. 2022, 7, 131−141

mouse macrophage Raw264.7 cells (Figure 5C,D) were incubated with various concentrations of H_2O_2 (15, 30, and 45 mM) or NaOCl (5, 10, and 15 mM) for 30 min, and the cell lysates were used to coat plates. After treating with anti-calmodulin antibody and tpMetROG, the RFIs were analyzed (Figure 5A−D). As expected, the RFIs for calmodulin gradually increased as the concentration of H_2O_2 or NaOCl used increased in all the tested cell lines.

LPS trigger the production of ROS in the macrophages by binding with toll-like receptor 4.[33] BLISA was applied to quantify the methionine oxidation of calmodulin in Raw264.7 cells stimulated with LPS for 6 and 16 h. The RFIs of calmodulin dramatically increased in LPS-stimulated cells for 6 and 16 h (Figure 5E). Therefore, these results demonstrate that the tpMetROG biosensor is able to quantify protein-specific methionine oxidation occurring in the cells.

Analysis of Methionine Oxidation in Calmodulin Obtained from Various Tissues of MsrB1 Knockout Mice Using BLISA. Methionine oxidation of calmodulin in animal tissues was analyzed using BLISA and tpMetROG. For this study, tissue samples of the small intestine, large intestine, brain, heart, liver, kidney, and lung were collected from MsrB1 knockout and WT mice. Interestingly, the RFIs for calmodulin were much higher in all organ tissues from MsrB1 knockout mice than those from WT mice (Figure 6). Consequently, this result demonstrates that the ablation of MsrB1 leads to severe methionine oxidation of calmodulin, thereby supporting the idea that MsrB1 is essential for maintaining the reduced state of methionine in proteins.

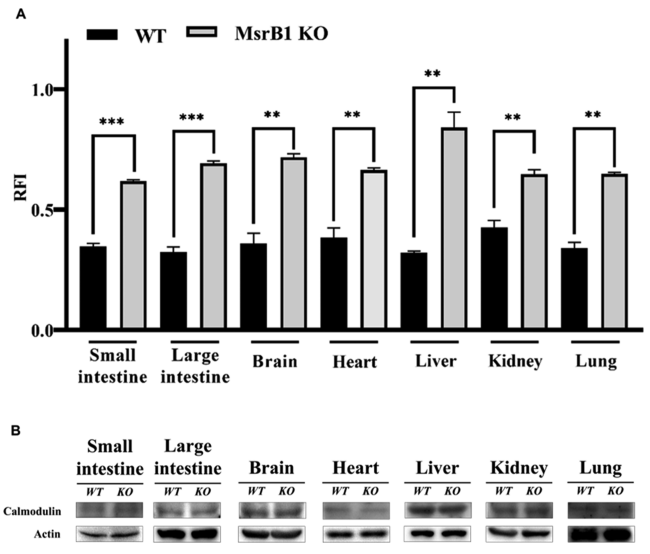

Figure 6. Quantitative analysis of calmodulin methionine oxidation in tissue extracts. Lysates of the small intestine, large intestine, large intestine, brain, heart, liver, kidney, and lung isolated from wild-type (WT) mice and MsrB1 knockout mice were used to compare the state of methionine oxidation of calmodulin. Organ extracts were coated in a plate, incubated with an anti-calmodulin (1:1000; Covance) antibody, followed by sensing using tpMetROG. (A) RFI of tpMetROG in immunoassay according to MsrB1 knockout and WT mice organ extracts. (B) Expression level of calmodulin in each organ was analyzed by western blot in MsrB1 knockout and WT mice. Data are presented as means ± SD and are representative of three replicates (A). $^{**}p < 0.01$ and $^{***}p < 0.001$; ns, not significant, as determined by the two-tailed paired *t*-test.

DISCUSSION

Oxidation of methionine residues often leads to structural abnormalities in protein and their malfunction. Therefore, it is critical to quantitatively measure the methionine oxidation status of proteins under various physiological conditions. Recently, two strategies were used to quantify the amount of methionine sulfoxide residues in proteins *in vivo*; the LC−MS using an isotope labeling with ^{18}O[34] and the fluorescence-based biosensor using cpYFP.[25] However, these methods have limitations in terms of complexity and the lack of specificity. In particular, considering that the oxidation of specific methionine residues in proteins, and not all methionines, is associated with the changes in protein functions, it is essential to quantify oxidation of a specific methionine residue within a protein. In this regard, the tpMetROG biosensor is an advanced tool that employs a fluorescent biosensor and antibodies against specific proteins, allowing for quantifying methionine oxidation of target proteins; it could be applied for any proteins if specific antibodies are available. Accurate analysis of methionine sulfoxide residues in specific proteins using LC−MS/MS has been challenging due to a high degree of spontaneous methionine oxidation during sample preparation. However, the immunosorbent assay using tpMetROG adopted the sampling process that does not require incubation with buffers containing methanol or heating, thereby preventing the spontaneous methionine oxidation.

Calmodulin is a multifunctional calcium-binding protein expressed in all eukaryotic cells.[35] Upon calcium binding, calmodulin undergoes conformational changes, which facilitate its interaction with various target proteins such as the kinases, phosphatases, phosphodiesterases, and ion channels.[35,36] However, oxidation of the methionine residues of calmodulin also leads to conformational changes that allow interaction with various target proteins without binding calcium.[37−40] The tpMetROG biosensor was able to quantify the oxidation of methionine residues in calmodulin under oxidative stress. Therefore, this biosensor can potentially be used to predict the changes in calmodulin functions associated with methionine oxidation. Many proteins, such as nitrogen assimilation transcription factor nirA (NirA), nuclear factor of κ B inhibitor α, HypT, CaMKII, actin, and calcineurin are functionally altered by reversible oxidation and reduction of methionine residues causing structural changes or altered interactions.[41] In particular, the two conserved methionine residues of actin are stereoselectively oxidized to methionine-*R*-sulfoxide by MICALs, which results in actin depolymerization. The tpMetROG biosensor allows us to understand the functional role of oxidation and reduction of methionine residues and conducting research on methionine residues in proteins as the potential regulators of cellular functions under various physiological conditions.

However, this novel biosensor still has some limitations. Currently, its application is limited to *in vitro* analysis. *In vivo* analysis such as live-cell imaging and immunohistochemistry should be developed to expand its use and contribution to various biological studies for better understanding the association of methionine oxidation and functional regulation within a specific protein. Also, this sensor is devised for quantifying the relative change of methionine oxidation in a specific protein, whereas the absolute value of methionine oxidation in a single protein cannot be analyzed in the present way. To make this possible, analysis of the number of

https://doi.org/10.1021/acssensors.1c01819
ACS Sens. 2022, 7, 131−141

methionine oxidation in a specific protein by using LC−MS/MS can be applied to examine the correlation of the number of methionine oxidation and fluorescence intensity. Future study will be conducted to overcome this hurdle of tpMetROG sensors in order to expand its application.

CONCLUSIONS

We developed the recombinant fluorescence-based sensor that includes MsrB, cpYFP, Trx3, and protein G. This sensor could successfully replace the secondary antibody to measure the oxidation of methionine residues of specific proteins in an immunosorbent assay, BLISA. In particular, methionine oxidation of calmodulin upon oxidative stress could be quantified in cells and tissues. For future research, this advanced tool would be useful for studying mechanisms linking methionine oxidation to changes in the function of various proteins. We need to consider the extended application of this biosensor, beyond the immunosorbent assay, as a versatile tool.

ASSOCIATED CONTENT

Supporting Information

The Supporting Information is available free of charge at https://pubs.acs.org/doi/10.1021/acssensors.1c01819.

pH dependence of tpMetROG, kinetic reactivity and pH dependence of tpMetROG, oligonucleotides used in this study, and *de novo* synthesized DNA sequences (PDF)

AUTHOR INFORMATION

Corresponding Authors

Ji Hyung Kim − *Department of Biotechnology, College of Life Sciences and Biotechnology, Korea University, Seoul 02841, Republic of Korea*; Email: jay_kim@korea.ac.kr

Byung Cheon Lee − *Department of Biotechnology, College of Life Sciences and Biotechnology, Korea University, Seoul 02841, Republic of Korea*; orcid.org/0000-0003-1467-1940; Email: cheonii@korea.ac.kr

Authors

Hae Min Lee − *Department of Biotechnology, College of Life Sciences and Biotechnology, Korea University, Seoul 02841, Republic of Korea*

Dong Wook Choi − *Department of Biochemistry, College of Natural Sciences, Chungnam National University, Daejeon 34134, Republic of Korea*

Seahyun Kim − *Department of Biotechnology, College of Life Sciences and Biotechnology, Korea University, Seoul 02841, Republic of Korea*

Aro Lee − *Department of Biotechnology, College of Life Sciences and Biotechnology, Korea University, Seoul 02841, Republic of Korea*

Minseo Kim − *Department of Biotechnology, College of Life Sciences and Biotechnology, Korea University, Seoul 02841, Republic of Korea*

Yeon Jin Roh − *Department of Biotechnology, College of Life Sciences and Biotechnology, Korea University, Seoul 02841, Republic of Korea*

Young Ho Jo − *Department of Biotechnology, College of Life Sciences and Biotechnology, Korea University, Seoul 02841, Republic of Korea*

Hwa Yeon Cho − *Department of Biotechnology, College of Life Sciences and Biotechnology, Korea University, Seoul 02841, Republic of Korea*

Ho-Jae Lee − *Department of Biotechnology, College of Life Sciences and Biotechnology, Korea University, Seoul 02841, Republic of Korea*

Seung-Rock Lee − *Department of Biochemistry, Research Center for Aging and Geriatrics, Chonnam National University Medical School, Gwangju 61186, Republic of Korea*

Lionel Tarrago − *INRAE, Aix Marseille University, BBF, Marseille F13108, France*

Vadim N. Gladyshev − *Division of Genetics, Department of Medicine, Brigham and Women's Hospital, Harvard Medical School, Boston, Massachusetts 02215, United States*

Complete contact information is available at: https://pubs.acs.org/10.1021/acssensors.1c01819

Author Contributions

J.H.K. and B.C.L. conceived and supervised the research. H.M.L. designed the experiment and carried out the experiments with support from S.K., A.L., M.K., Y.J.R., Y.H.J., H.Y.C., and H.-J.L. The manuscript was written by H.M.L., D.W.C., L.T., V.N.G., J.H.K., and B.C.L. All authors reviewed and edited the manuscript.

Notes

The authors declare the following competing financial interest(s): The authors have filed a patent application relating to the technology.

ACKNOWLEDGMENTS

This work was supported by the National Research Foundation of Korea (NRF) grants (2021R1A2C4086540) funded by the Korean government (Ministry of Science, ICT & Future Planning) to B.C.L.

ABBREVIATIONS

MsrB, methionine sulfoxide reductase B; cpYFP, circularly permuted yellow fluorescent protein; ROS, reactive oxygen species; Met, methionine; MetSO, methionine-*S*-sulfoxide; MetRO, methionine-*R*-sulfoxide; CaMKII, calcium-/calmodulin-dependent protein kinase II; HypT, hypochlorite-responsive transcription factor; MICAL, molecule interacting with CasL; NFI, normalized fluorescence intensity; RFI, relative fluorescence intensity; MRP, methionine-rich protein; IgG, immunoglobulin G; BLISA, biosensor-linked immunosorbent assay; NirA, nitrogen assimilation transcription factor nirA; IkBα, nuclear factor of κ B inhibitor α

REFERENCES

(1) Muthukumar, K.; Nachiappan, V. Cadmium-induced oxidative stress in Saccharomyces cerevisiae. *Indian J. Biochem. Biophys.* **2010**, *47*, 383−387.

(2) Zhao, G.; Yu, R.; Deng, J.; Zhao, Q.; Li, Y.; Joo, M.; van Breemen, R. B.; Christman, J. W.; Xiao, L. Pivotal role of reactive oxygen species in differential regulation of lipopolysaccharide-induced prostaglandins production in macrophages. *Mol. Pharmacol.* **2013**, *83*, 167−178.

(3) Nita, M.; Grzybowski, A. The Role of the Reactive Oxygen Species and Oxidative Stress in the Pathomechanism of the Age-Related Ocular Diseases and Other Pathologies of the Anterior and Posterior Eye Segments in Adults. *Oxid. Med. Cell. Longevity* **2016**, *2016*, 3164734.

(4) Tabner, B. J.; El-Agnaf, O. M.; German, M. J.; Fullwood, N. J.; Allsop, D. Protein aggregation, metals and oxidative stress in neurodegenerative diseases. *Biochem. Soc. Trans.* **2005**, *33*, 1082−1086.
(5) Catalá, A. Lipid peroxidation of membrane phospholipids generates hydroxy-alkenals and oxidized phospholipids active in physiological and/or pathological conditions. *Chem. Phys. Lipids* **2009**, *157*, 1−11.
(6) Boschi-Muller, S.; Olry, A.; Antoine, M.; Branlant, G. The enzymology and biochemistry of methionine sulfoxide reductases. *Biochim. Biophys. Acta* **2005**, *1703*, 231−238.
(7) Kaya, A.; Lee, B. C.; Gladyshev, V. N. Regulation of protein function by reversible methionine oxidation and the role of selenoprotein MsrB1. *Antioxid. Redox Signaling* **2015**, *23*, 814−822.
(8) Henry, C.; Loiseau, L.; Vergnes, A.; Vertommen, D.; Mérida-Floriano, A.; Chitteni-Pattu, S.; Wood, E. A.; Casadesús, J.; Cox, M. M.; Barras, F.; Ezraty, B. Redox controls RecA protein activity via reversible oxidation of its methionine residues. *Elife* **2021**, *10*, No. e63747.
(9) Nicklow, E. E.; Sevier, C. S. Activity of the yeast cytoplasmic Hsp70 nucleotide-exchange factor Fes1 is regulated by reversible methionine oxidation. *J. Biol. Chem.* **2020**, *295*, 552−569.
(10) Wang, Q.; Hernández-Ochoa, E. O.; Viswanathan, M. C.; Blum, I. D.; Do, D. C.; Granger, J. M.; Murphy, K. R.; Wei, A.-C.; Aja, S.; Liu, N.; Antonescu, C. M.; Florea, L. D.; Talbot, C. C.; Mohr, D.; Wagner, K. R.; Regot, S.; Lovering, R. M.; Gao, P.; Bianchet, M. A.; Wu, M. N.; Cammarato, A.; Schneider, M. F.; Bever, G. S.; Anderson, M. E. CaMKII oxidation is a critical performance/disease trade-off acquired at the dawn of vertebrate evolution. *Nat. Commun.* **2021**, *12*, 3175.
(11) Erickson, J. R.; Joiner, M.-l. A.; Guan, X.; Kutschke, W.; Yang, J.; Oddis, C. V.; Bartlett, R. K.; Lowe, J. S.; O'Donnell, S. E.; Aykin-Burns, N.; Zimmerman, M. C.; Zimmerman, K.; Ham, A.-J. L.; Weiss, R. M.; Spitz, D. R.; Shea, M. A.; Colbran, R. J.; Mohler, P. J.; Anderson, M. E. A dynamic pathway for calcium-independent activation of CaMKII by methionine oxidation. *Cell* **2008**, *133*, 462−474.
(12) Drazic, A.; Miura, H.; Peschek, J.; Le, Y.; Bach, N. C.; Kriehuber, T.; Winter, J. Methionine oxidation activates a transcription factor in response to oxidative stress. *Proc. Natl. Acad. Sci. U.S.A.* **2013**, *110*, 9493−9498.
(13) Dalle-Donne, I.; Rossi, R.; Giustarini, D.; Gagliano, N.; Di Simplicio, P.; Colombo, R.; Milzani, A. Methionine oxidation as a major cause of the functional impairment of oxidized actin. *Free Radical Biol. Med.* **2002**, *32*, 927−937.
(14) Grintsevich, E. E.; Yesilyurt, H. G.; Rich, S. K.; Hung, R.-J.; Terman, J. R.; Reisler, E. F-actin dismantling through a redox-driven synergy between Mical and cofilin. *Nat. Cell Biol.* **2016**, *18*, 876−885.
(15) Lee, B. C.; Lee, S.-G.; Choo, M.-K.; Kim, J. H.; Lee, H. M.; Kim, S.; Fomenko, D. E.; Kim, H.-Y.; Park, J. M.; Gladyshev, V. N. Selenoprotein MsrB1 promotes anti-inflammatory cytokine gene expression in macrophages and controls immune response in vivo. *Sci. Rep.* **2017**, *7*, 5119.
(16) Lee, B. C.; Péterfi, Z.; Hoffmann, F. W.; Moore, R. E.; Kaya, A.; Avanesov, A.; Tarrago, L.; Zhou, Y.; Weerapana, E.; Fomenko, D. E.; Hoffmann, P. R.; Gladyshev, V. N. MsrB1 and MICALs regulate actin assembly and macrophage function via reversible stereoselective methionine oxidation. *Mol. Cell* **2013**, *51*, 397−404.
(17) McCarthy, M. R.; Thompson, A. R.; Nitu, F.; Moen, R. J.; Olenek, M. J.; Klein, J. C.; Thomas, D. D. Impact of methionine oxidation on calmodulin structural dynamics. *Biochem. Biophys. Res. Commun.* **2015**, *456*, 567−572.
(18) Klein, J. C.; Moen, R. J.; Smith, E. A.; Titus, M. A.; Thomas, D. D. Structural and functional impact of site-directed methionine oxidation in myosin. *Biochemistry* **2011**, *50*, 10318−10327.
(19) Shao, B.; Cavigiolio, G.; Brot, N.; Oda, M. N.; Heinecke, J. W. Methionine oxidation impairs reverse cholesterol transport by apolipoprotein A-I. *Proc. Natl. Acad. Sci. U.S.A.* **2008**, *105*, 12224−12229.
(20) Sun, G.; Anderson, V. E. Prevention of artifactual protein oxidation generated during sodium dodecyl sulfate-gel electrophoresis. *Electrophoresis* **2004**, *25*, 959−965.
(21) Shipman, J. T.; Go, E. P.; Desaire, H. Method for Quantifying Oxidized Methionines and Application to HIV-1 Env. *J. Am. Soc. Mass Spectrom.* **2018**, *29*, 2041−2047.
(22) Bettinger, J. Q.; Welle, K. A.; Hryhorenko, J. R.; Ghaemmaghami, S. Quantitative Analysis of in Vivo Methionine Oxidation of the Human Proteome. *J. Proteome Res.* **2020**, *19*, 624−633.
(23) Ghesquière, B.; Gevaert, K. Proteomics methods to study methionine oxidation. *Mass Spectrom. Rev.* **2014**, *33*, 147−156.
(24) Liu, H.; Ponniah, G.; Neill, A.; Patel, R.; Andrien, B. Accurate determination of protein methionine oxidation by stable isotope labeling and LC-MS analysis. *Anal. Chem.* **2013**, *85*, 11705−11709.
(25) Tarrago, L.; Péterfi, Z.; Lee, B. C.; Michel, T.; Gladyshev, V. N. Monitoring methionine sulfoxide with stereospecific mechanism-based fluorescent sensors. *Nat. Chem. Biol.* **2015**, *11*, 332−338.
(26) Belousov, V. V.; Fradkov, A. F.; Lukyanov, K. A.; Staroverov, D. B.; Shakhbazov, K. S.; Terskikh, A. V.; Lukyanov, S. Genetically encoded fluorescent indicator for intracellular hydrogen peroxide. *Nat. Methods* **2006**, *3*, 281−286.
(27) Liang, X.; Kaya, A.; Zhang, Y.; Le, D. T.; Hua, D.; Gladyshev, V. N. Characterization of methionine oxidation and methionine sulfoxide reduction using methionine-rich cysteine-free proteins. *BMC Biochem.* **2012**, *13*, 21.
(28) Péterfi, Z.; Tarrago, L.; Gladyshev, V. N. Practical guide for dynamic monitoring of protein oxidation using genetically encoded ratiometric fluorescent biosensors of methionine sulfoxide. *Methods* **2016**, *109*, 149−157.
(29) Fomenko, D. E.; Novoselov, S. V.; Natarajan, S. K.; Lee, B. C.; Koc, A.; Carlson, B. A.; Lee, T.-H.; Kim, H.-Y.; Hatfield, D. L.; Gladyshev, V. N. MsrB1 (Methionine-R-sulfoxide Reductase 1) Knock-out Mice Roles of MsrB1 in Redox Regulation and Identification of a Novel Selenoprotein Form. *J. Biol. Chem.* **2009**, *284*, 5986−5993.
(30) Kim, J.; Lee, H.; Roh, Y. J.; Kim, H.-u.; Shin, D.; Kim, S.; Son, J.; Lee, A.; Kim, M.; Park, J.; Hwang, S. Y.; Kim, K.; Lee, Y. K.; Jung, H. S.; Hwang, K. Y.; Lee, B. C. Structural and kinetic insights into flavin-containing monooxygenase and calponin-homology domains in human MICAL3. *Iucrj* **2020**, *7*, 90−99.
(31) Sasaki, A.; Tsukasaki, Y.; Komatsuzaki, A.; Sakata, T.; Yasuda, H.; Jin, T. Recombinant protein (EGFP-Protein G)-coated PbS quantum dots for in vitro and in vivo dual fluorescence (visible and second-NIR) imaging of breast tumors. *Nanoscale* **2015**, *7*, 5115−5119.
(32) Choi, D. W.; Roh, Y. J.; Kim, S.; Lee, H. M.; Kim, M.; Shin, D.; Park, J. H.; Cho, Y.; Park, H. H.; Ok, Y. S.; Kang, D.; Kim, J. H.; Tarrago, L.; Danial, N. N.; Gladyshev, V. N.; Min, P. K.; Lee, B. C. Development of a novel fluorescent biosensor for dynamic monitoring of metabolic methionine redox status in cells and tissues. *Biosens. Bioelectron.* **2021**, *178*, 113031.
(33) Zhao, G.; Yu, R.; Deng, J.; Zhao, Q.; Li, Y.; Joo, M.; van Breemen, R. B.; Christman, J. W.; Xiao, L. Pivotal Role of Reactive Oxygen Species in Differential Regulation of Lipopolysaccharide-Induced Prostaglandins Production in Macrophages. *Mol. Pharmacol.* **2013**, *83*, 167−178.
(34) Liu, H.; Ponniah, G.; Neill, A.; Patel, R.; Andrien, B. Accurate Determination of Protein Methionine Oxidation by Stable Isotope Labeling and LC-MS Analysis. *Anal. Chem.* **2013**, *85*, 11705−11709.
(35) Chin, D.; Means, A. R. Calmodulin: a prototypical calcium sensor. *Trends Cell Biol.* **2000**, *10*, 322−328.
(36) Vougier, S.; Mary, J.; Dautin, N.; Vinh, J.; Friguet, B.; Ladant, D. Essential role of methionine residues in calmodulin binding to Bordetella pertussis adenylate cyclase, as probed by selective oxidation and repair by the peptide methionine sulfoxide reductases. *J. Biol. Chem.* **2004**, *279*, 30210−30218.
(37) Heiby, J. C.; Goretzki, B.; Johnson, C. M.; Hellmich, U. A.; Neuweiler, H. Methionine in a protein hydrophobic core drives tight

interactions required for assembly of spider silk. *Nat. Commun.* **2019**, *10*, 4378.
(38) Bartlett, R. K.; Urbauer, R. J. B.; Anbanandam, A.; Smallwood, H. S.; Urbauer, J. L.; Squier, T. C. Oxidation of Met(144) and Met(145) in calmodulin blocks calmodulin dependent activation of the plasma membrane Ca-ATPase. *Biochemistry* **2003**, *42*, 3231−3238.
(39) McCarthy, M. R.; Thompson, A. R.; Nitu, F.; Moen, R. J.; Olenek, M. J.; Klein, J. C.; Thomas, D. D. Impact of methionine oxidation on calmodulin structural dynamics. *Biochem. Biophys. Res. Commun.* **2015**, *456*, 567−572.
(40) Marimoutou, M.; Springer, D. A.; Liu, C. Y.; Kim, G.; Levine, R. L. Oxidation of Methionine 77 in Calmodulin Alters Mouse Growth and Behavior. *Antioxidants* **2018**, *7*, 140.
(41) Aledo, J. C. Methionine in proteins: The Cinderella of the proteinogenic amino acids. *Protein Sci.* **2019**, *28*, 1785−1796.

https://doi.org/10.1021/acssensors.1c01819
ACS Sens. 2022, 7, 131−141